Low-lying collective states in $^{98-106}$Ru isotopes studied using a microscopic anharmonic vibrator approach

J. Kotila and J. Suhonen
Department of Physics, University of Jyväskylä, P.O. Box 35, FIN-40014, Jyväskylä, Finland

D. S. Delion
National Institute of Physics and Nuclear Engineering, P.O. Box MG-6, Bucharest Măgurele, Romania
(Received 1 August 2003; published 25 November 2003)

Anharmonic features of the low-lying collective states in the $^{98-106}$Ru isotopes have been investigated systematically by using the microscopic anharmonic vibrator approach (MAVA). MAVA is based on a realistic microscopic *G*-matrix Hamiltonian, only slightly renormalized in the adopted large realistic single-particle spaces. This Hamiltonian is used to derive equations of motion for the mixing of one- and two-phonon degrees of freedom starting from collective phonons of the quasiparticle random-phase approximation. Analysis of the level energies and the electric quadrupole decays of the two-phonon type of states indicates that ^{100}Ru can be interpreted as being a transitional nucleus between the spherical anharmonic vibrator ^{98}Ru and the quasirotational heavier $^{102-106}$Ru isotopes.

DOI: 10.1103/PhysRevC.68.054322 PACS number(s): 21.60.Ev, 21.60.Jz, 23.20.Lv, 27.60.+j

I. INTRODUCTION

It is well known that spherical and nearly spherical nuclei exhibit low-energy collective spectra with vibrational-like states below the pairing gap. The pairing gap is produced by the short-range nucleon correlations whereas the collective features emerge from the long-range residual interaction. Investigation of these collective states as collective phonons and their multiples has been of extensive interest both experimentally and theoretically. In quasiparticle description of the superfluid nuclei these vibrational phonons have been described as coherent combinations of two-quasiparticle states, the residual interaction causing these phonons to fall far below other two-quasiparticle states, which remain above the pairing gap. Collective (an)harmonic vibrational states built of two or even three of these phonons (two-phonon and three-phonon states) have been the subject of systematic phenomenological analysis, e.g., in Ref. [1]. Microscopic description of these multiphonon states involves configuration mixing of two-quasiparticle, four-quasiparticle, six-quasiparticle, etc., degrees of freedom.

From the microscopic point of view the low-energy collective phonons of the medium-heavy and heavy open-shell nuclei are conveniently described within the framework of the quasiparticle random-phase approximation (QRPA), which in our case describes harmonic small-amplitude vibrations around a spherical nuclear shape [2–4]. These collective low-energy solutions of the QRPA equations can be combined to multiphonon states, e.g., in the multistep shell model [5,6], in the quasiparticle phonon model of Soloviev [7], and in the extended QRPA approach [8]. In our recent theoretical framework [9], the microscopic anharmonic vibrator approach (MAVA), the one-phonon states are based on the QRPA phonons, and the one-phonon and two-phonon states are allowed to interact among each other through the H_{31} part of the quasiparticle representation of the residual two-body Hamiltonian. In this way the degeneracy of the two-phonon triplet is broken, partly by the H_{31} operator and partly by the metric matrix containing the overlaps between the two-particle states. It is worth pointing out that the MAVA is a completely microscopic scheme derived by using the equations-of-motion approach of Rowe [3]. The inclusion of the Pauli principle is taken care of by diagonalizing the metric matrix thus creating a complete orthonormal basis and then diagonalizing the residual Hamiltonian in this basis.

In recent years, several calculations of spectra of even-even ruthenium nuclei have been performed within the framework of the interacting boson model (IBA) and its extensions. In the original version of the IBA, IBA-1, no distinction is made between neutron and proton bosons. The proton-neutron interacting boson model IBA-2, one of the extensions of the IBA, distinguishes proton and neutron degrees of freedom. The consistent-*Q* formalism (CQF) is another development of the IBA as also is the extended consistent-*Q* formalism (ECQF) [10].

In experimental paper by Hirata *et al.* [11] a comparison between their determination of the $B(E2)$ values and the results of IBA-1 and IBA-2 calculations was made. The $B(E2)$ values calculated in the framework of the IBA-1 [12,13] are significantly lower than the experimental values. The $B(E2)$ values obtained from IBA-2 calculations by Van Isacker *et al.* [14] are systematically higher than the experimental mean values, whereas the $B(E2)$ values obtained from IBA-2 calculations by Giannatiempo *et al.* [15] are systematically lower.

In their paper, Van Isacker *et al.* [14] have also paid special attention to the occurrence of 0^+ states which are not reproduced by their calculation. In ^{100}Ru and ^{102}Ru the 0_2^+ states are suspected to be intruder states of some kind. For the heavier isotopes the 0_2^+ states are considered to be rotational collective states. Contrary to that, in the study of Giannatiempo *et al.* [15] the excitation energy of the 0_2^+ state is well reproduced all along the isotopic chain. They also sug-

TABLE I. Basic data for the discussed ruthenium nuclei. The pairing gaps (Δ) and the corresponding pairing strengths ($g_{\rm pair}$) for protons and neutrons are given in columns 2–5. In columns 6 and 7 the particle-hole parameters of the QRPA are given for the 2^+ and 4^+ multipoles. In column 8 the experimental $B(E2;2_1^+\rightarrow 0_1^+)$ are given in Weisskopf units (W.u.), and finally, in column 9 we list the values of the corresponding polarization parameter for the effective proton and neutron charges.

A	Δ_p	Δ_n	$g_{\rm pair}^{(p)}$	$g_{\rm pair}^{(n)}$	$g_{ph}(2^+)$	$g_{ph}(4^+)$	$B(E2)_{\rm exp}$(W.u.)	χ
98	1.2006	1.5715	1.1354	1.1673	0.992	1.000	27.8(6)[a]	0.28
100	1.2701	1.5976	1.0638	1.1750	0.898	1.000	35.8(4)[b]	0.37
102	1.3512	1.6119	1.0265	1.1845	0.828	1.000	43.9(4)[c]	0.47
104	1.4164	1.5465	1.0543	1.1547	0.791	1.000	60(3)[d]	0.58
106	1.3375	1.3910	1.0295	1.0911	0.765	1.000		0.67

[a]Data from Ref. [38].
[b]Data from Ref. [39].
[c]Data from Ref. [42].
[d]Data from Ref. [40].

gest that the 0_2^+ state shows a rather pure full symmetry structure, without any mixed symmetry contributions, all along the chain.

In the CQF proposed by Warner and Casten [16], the original IBA-1 Hamiltonian is specified to contain exactly the operator used for the electric transitions. Use of this new Hamiltonian leads to a description of the transitional nuclei between the axially deformed SU(3) limit and the γ-unstable O(6) limit in terms of essentially only one free parameter [17]. However, in the study of Stachel *et al.* [18] the structure of even ruthenium isotopes was suggested, based on an analysis limited to the full symmetry states (IBA-1), to pertain to the U(5)-O(6) side of the Casten triangle [19]. Therefore, Bucurescu *et al.* [17] have applied in their study a formalism similar to the CQF to a more general Hamiltonian, which can also describe the U(5)-O(6) transition. This approach, called ECQF, gives an overall fit comparable to that of the IBA-2. Very recently, the $^{98-110}$Ru nuclei were analyzed in search of the $E(5)$ critical symmetry [20]. This symmetry should be found midway between the spherical vibrator and the γ-unstable rotor [21]. Another critical point symmetry $X(5)$ should be found midway between a spherical vibrator and an axially symmetric rotor [22].

In the present paper we perform a systematic analysis of the electric decay properties of the $^{98-106}$Ru nuclei by using the MAVA. A comparison of the calculated level energies with the IBA-1 results of Ref. [23] has been done. In this way we hope to learn about the systematic evolution of anharmonic effects and deformation along the ruthenium chain of isotopes. Our paper is organized as follows. In Sec. II we outline the necessary theoretical aspects and their numerical application to Ru isotopes. In Sec. III we review the results and discuss them. The conclusions are drawn in Sec. IV.

II. NUMERICAL APPLICATION TO RUTHENIUM ISOTOPES

We start our microscopic approach from a single-particle basis of a suitable size. In the present work we use eigenvalues of the spherical Woods-Saxon nuclear mean field with the Coulomb terms included using the parametrization of Ref. [24]. The single-particle wave functions are taken, however, to be eigenstates of a spherical harmonic oscillator with a suitable oscillator constant which is a good approximation for bound states in nuclei. We have chosen for the studied $^{98-106}$Ru isotopes a basis of ten proton and neutron single-particle levels around the proton and neutron Fermi surfaces, spanning the following valence space: pf-sdg-$h_{11/2}$ shells. The BCS occupation amplitudes and the QRPA eigenstates were calculated using as residual two-body interaction the G-matrix elements of the Bonn one-boson-exchange interaction [25]. Different channels of this interaction are scaled by constants as described in Refs. [26,27].

The pairing strength for protons and neutrons was adjusted by requiring the calculated pairing gaps to reproduce the empirical ones obtained from the proton and neutron separation energies [28]. The resulting pairing parameters, along with the used pairing gaps, have been listed in Table I. In this case the values $g_{\rm pair}^{(p)}=1.0$ and $g_{\rm pair}^{(n)}=1.0$ correspond to pairing matrix elements coming from the bare monopole part of the G matrix.

The G-matrix elements for the $J^\pi=2^+, 4^+$ multipoles in the QRPA calculations have been parametrized by two parameters [27], namely, the particle-hole parameter g_{ph} and the particle-particle parameter g_{pp}. Here the particle-particle part has practically no effect on the physical observables so that its value has been set to $g_{pp}=1.0$, corresponding to the bare G matrix. The value of the particle-hole parameter controls the energy of the lowest 2^+ and 4^+ states in the QRPA calculation. Thus this parameter can be used to control the position of the first 2^+ and second 4^+ states in the final theoretical spectrum. The adopted values of the g_{ph} parameters are listed in Table I. The available experimental data about the energies of the second 4^+ states are quite poor. Therefore, the parameter is chosen to be $g_{ph}(4^+)=1.0$ for all considered nuclei.

In our effective many-body framework the two-phonon states are built in terms of the QRPA degrees of freedom using the equations-of-motion technique of Rowe [3]:

$$[\hat{H}, \Gamma^\dagger_{a_4\alpha_4\mu_4}] = \mathcal{E}_{a_4\alpha_4}\Gamma^\dagger_{a_4\alpha_4\mu_4}, \tag{2.1}$$

where the ansatz wave function has been chosen to be of the form

TABLE II. Experimental and theoretical ratios $R_{if}(E2)$ of Eq. (3.1) for the $^{98-102}$Ru isotopes.

	^{98}Ru[a]		^{100}Ru[b]		^{102}Ru[c]	
Transition	Theor	Expt.	Theor	Expt.	Theor	Expt.
$2_1^+ \to 0_1^+$	1	1	1	1	1	1
$0_{2\text{-}ph}^+ \to 2_1^+$	1.736		1.603	1.0(2)	1.432	0.80(9)
$2_{2\text{-}ph}^+ \to 2_1^+$	1.650	1.6(7)	1.438	0.64(13)	1.433	0.62(8)
$4_{2\text{-}ph}^+ \to 2_1^+$	1.499	1.5(3)	1.338	1.51(8)	1.231	1.5(3)
$2_{2\text{-}ph}^+ \to 0_1^+$	0.034	0.036(15)	0.061	0.041(6)	0.050	0.0250(8)

[a]Data from Ref. [38].
[b]Data from Ref. [39].
[c]Data from Ref. [42].

$$\Gamma^\dagger_{a_4\alpha_4\mu_4} = \sum_{a_2} Z_1(a_2;a_4\alpha_4) Q^\dagger_{a_2\alpha_4\mu_4} \tag{2.2}$$

$$+ \sum_{a_2\alpha_2 \leqslant b_2\beta_2} Z_2(a_2\alpha_2 b_2\beta_2;a_4\alpha_4)(Q^\dagger_{a_2\alpha_2} Q^\dagger_{b_2\beta_2})_{\alpha_4\mu_4}, \tag{2.3}$$

containing a one-phonon part with quantum numbers $a_2\alpha_4\mu_4$ and a two-phonon part coupled to a total angular momentum (and parity) α_4 with z-projection μ_4. The quantum numbers a_2 and a_4 indicate the eigenvalue index of a QRPA phonon and the final diagonalized MAVA wave function, respectively.

Equation (2.1) together with ansatz (2.2) lead to a system of equations given explicitly in Ref. [9]. These equations contain, as a relevant part, the metric matrix consisting of overlaps between all the two-phonon combinations included in the calculations. This metric matrix is angular-momentum dependent and hence contributes to the splitting of the two-phonon-like MAVA states. Diagonalization of the metric matrix preserves the Pauli principle as described in detail in Ref. [9]. It has to be mentioned that the results for the five lowest calculated MAVA states (2_1^+, $0_{2\text{-}ph}^+$, $2_{2\text{-}ph}^+$, $4_{2\text{-}ph}^+$, and 4_2^+) depend on the number of the QRPA 2^+ and 4^+ phonons included into the ansatz wave function (2.2) and the subsequent diagonalization of the eigenvalue problem. According to our calculations it is enough to take five lowest QRPA phonons of both of these angular momenta to achieve stable energies and wave functions for the above mentioned MAVA states. All the results presented in the following section have been calculated using this number of the QRPA phonons.

In the MAVA, the metric matrix plays an important role in the theoretical expressions for the electric decay amplitudes [9]. These amplitudes can be used to produce the reduced electric quadrupole decay probabilities, $B(E2)$, to be compared with the experimental data. For this comparison we adopted proton and neutron effective charges, e_p and e_n, and used the experimental $B(E2;2_1^+ \to 0_1^+)$ value, also listed in Table I, to fix their value, by using the relations $e_p=(1+\chi)e$,$e_n=\chi e$ (see, e.g., Ref. [24]). The polarization parameter χ is listed in the last column of Table I. As the mass-number A increases, larger and larger effective charges are needed to reproduce the experimental $B(E2)$. However, for the nucleus $A=106$ there are no experimental data available so that the χ value had to be extrapolated.

III. RESULTS AND DISCUSSION

We present our results for the energies and the $B(E2)$ values in Tables II and III, and Figs. 1–8. Figures 1–5 show the theoretical and experimental energies of the 2_1^+ state and the two-phonon triplet of $^{98-106}$Ru. For comparison, Figs. 1–4 show also the results of the IBA-1 calculations of Kern *et al.* [23]. The decomposition of the five lowest states obtained by using our theory in terms of the QRPA phonons and their two-phonon combinations can be seen in Figs. 6 and 7. Figure 8 presents the evolution, as functions of the mass number, of the energies for the QRPA (dots) 2_1^+,4_1^+,2_2^+,4_2^+ phonons and the corresponding MAVA states (stars) containing the QRPA 2_1^+,4_1^+,2_2^+,4_2^+ phonons as main components. For completeness, we plot also the evolution of the two-phonon states of the MAVA.

The ruthenium isotopes have been a subject of a variety of theoretical model analyses along the years [14,15,17,18,23,29–37]. The key in the many discussions is the phenomena of shape transitions and shape coexistence along the isotopic chain of ruthenium isotopes. Frank [34] suggests a transition from spherical to a γ-unstable structure, whereas Troltenier *et al.* [32] discuss a spherical-triaxial transition. In papers by Zajaç *et al.* and Bucurescu *et al.* [29,17] the conclusion is that the heavier ruthenium nuclei are in general triaxial but γ soft or very γ soft. Because of the postulated shape transition, the Ru nuclei with $98<A<102$ are thought to be soft vibrators and those with

TABLE III. The same as Table II for the $^{104-106}$Ru isotopes.

	^{104}Ru[a]		^{106}Ru	
Transition	Theor	Expt.	Theor	Expt.
$2_1^+ \to 0_1^+$	1	1	1	
$0_{2\text{-}ph}^+ \to 2_1^+$	1.297	0.42(7)	1.296	
$2_{2\text{-}ph}^+ \to 2_1^+$	1.317	0.63(11)	1.330	
$4_{2\text{-}ph}^+ \to 2_1^+$	1.141	1.2(3)	1.174	
$2_{2\text{-}ph}^+ \to 0_1^+$	0.068	0.035(9)	0.086	

[a]Data from Ref. [40].

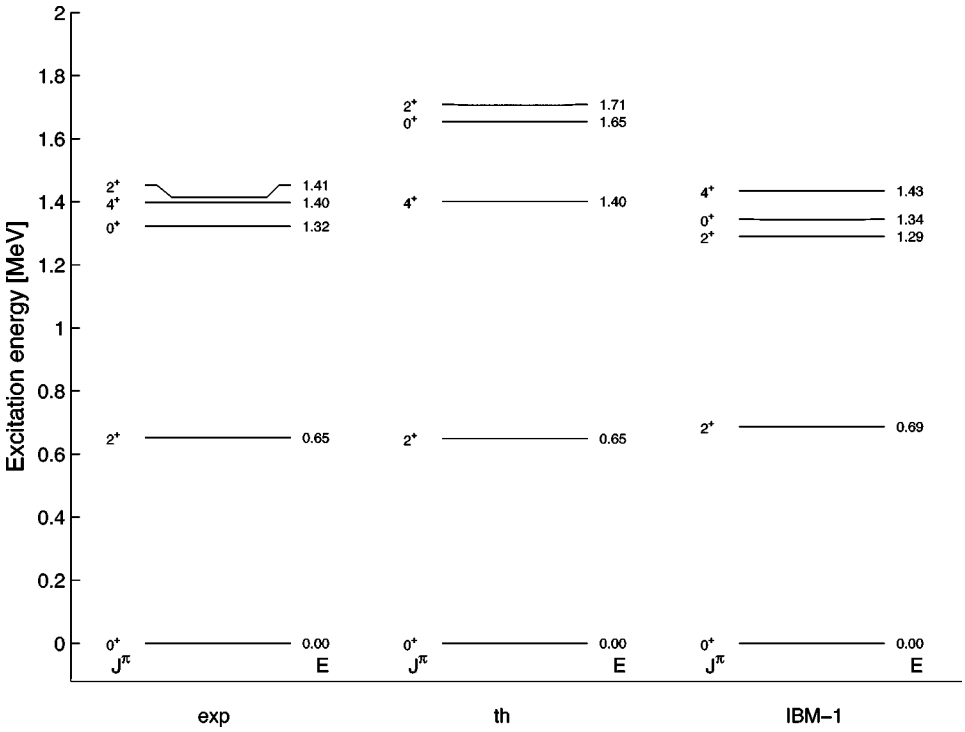

FIG. 1. Theoretical and experimental [38] low-energy spectra of ^{98}Ru.

$A>104$ quasirotors, whereas $A=104$ is a transitional nucleus forming a zone between soft vibrators on one side and nearly deformed rotors on the other side [30,31]. Among these studies the Ru isotopes have been investigated extensively within the IBA-1 model because its versatile symmetry structure is considered to be particularly appropriate for treating transitional nuclei.

Survey of Figs. 1–4 shows that the IBA-1 [23] calculations give better numerical values for energies. On the other hand, our calculations give better correspondence with the experimental data when comparing the ordering of the states. Especially satisfying are the $4^+_{2\text{-}ph}$ states for $A=98,102$ and $0^+_{2\text{-}ph}$ states for $A=102,104$. In our calculations the two-phonon-like 4^+ state is always below the 2^+ state coinciding with the interpretation of Refs. [38–41] for the ^{98,100,104,106}Ru nuclei. For the ^{102}Ru nuclei our theoretical result contradicts the view of Ref. [42] where the two-phonon-like 2^+ and 4^+ states are separated only by 10 keV.

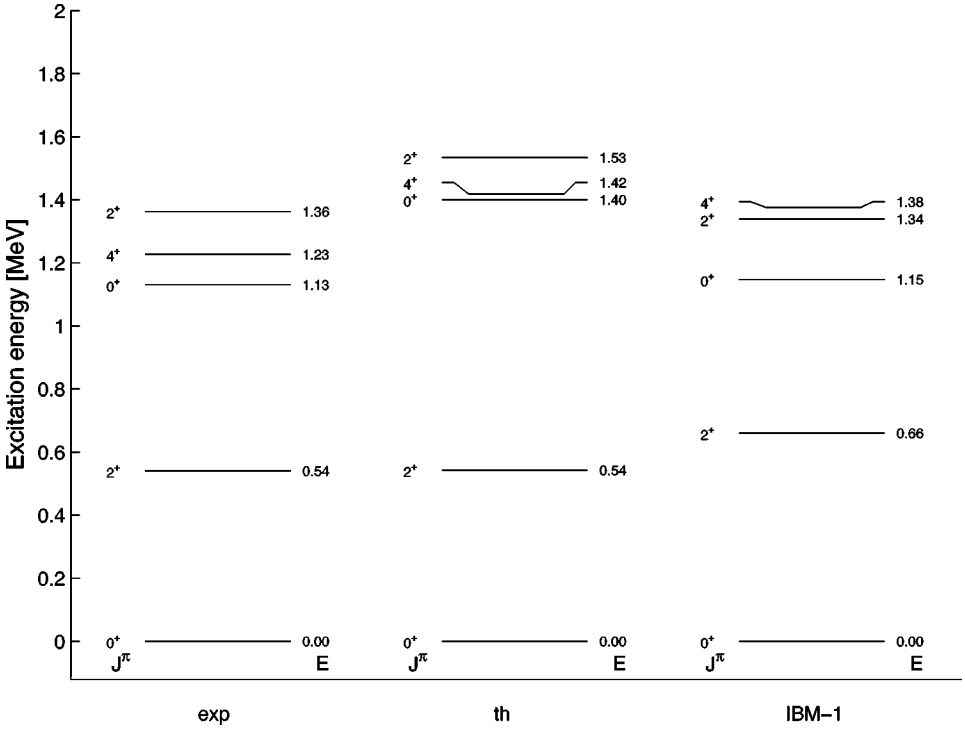

FIG. 2. Theoretical and experimental [39] low-energy spectra of ^{100}Ru.

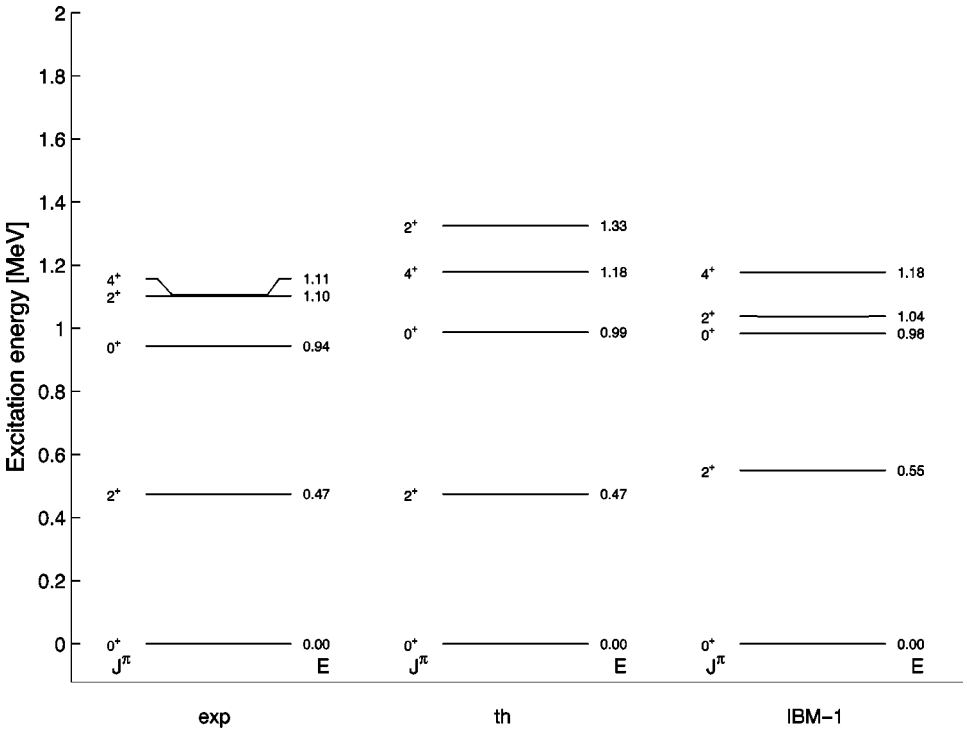

FIG. 3. Theoretical and experimental [40] low-energy spectra of ^{102}Ru.

However, our model does not reproduce the correct ordering of all the measured two-phonon members in the discussed ruthenium chain. The simple energetics of our model calculation can be interpreted as missing intruder degrees of freedom which could perturb our calculated wave functions. Also the presence of three-phonon states could affect the energies of the two-phonon states as happens in the case of the Cd isotopes [43]. Nevertheless, one has to bear in mind that although our calculation does not contain the three-phonon states and the deformed intruder degrees of freedom, it contains anharmonicities in any wanted amount, so that we are in a position to analyze the effects of such anharmonicities in a consistent way for the energies and the $B(E2)$ values.

The anharmonicities can be clearly seen in Figs. 6 and 7 where we have decomposed the five lowest theoretical MAVA levels into their one- and two-phonon components. From Fig. 6 one can see that the members of the two-phonon triplet $0_2^+, 2_2^+, 4_1^+$ have a large $(2_1^+ 2_1^+)_J$ component, thus sup-

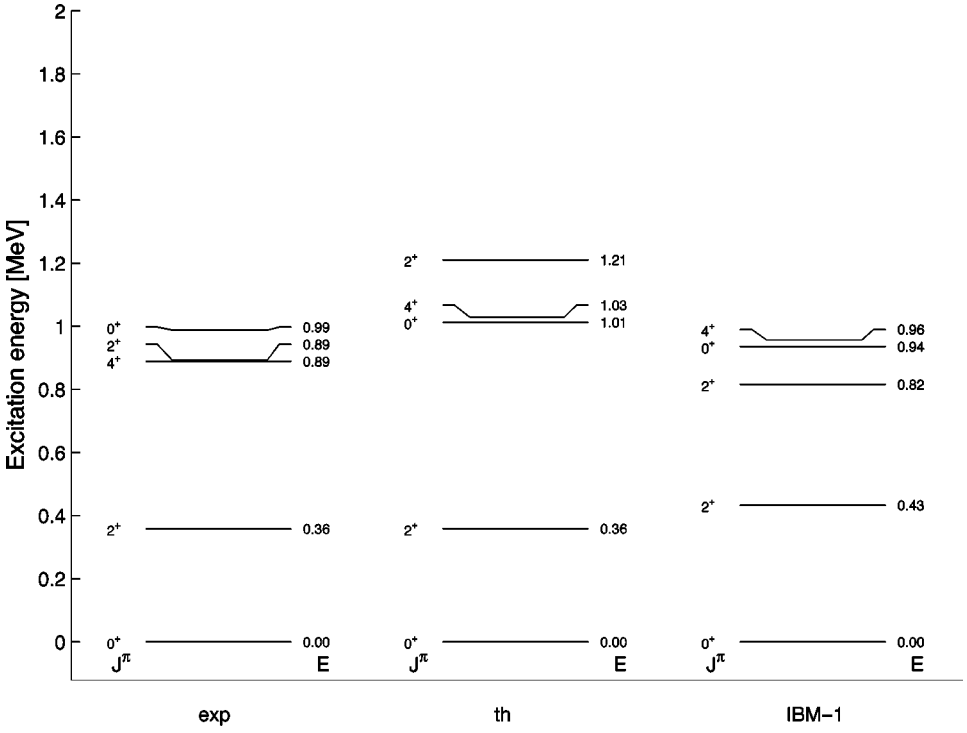

FIG. 4. Theoretical and experimental [41] low-energy spectra of ^{104}Ru.

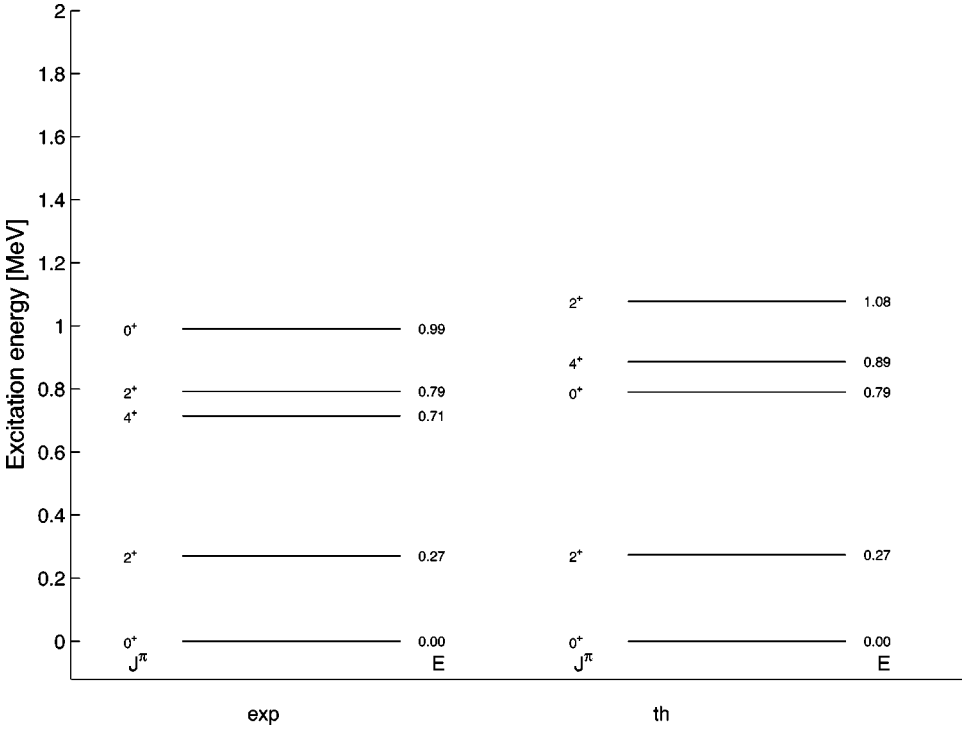

FIG. 5. Theoretical and experimental [42] low-energy spectra of ^{106}Ru.

porting the picture of a two-phonon vibrational state with anharmonicities showing up as other nonzero components of one-phonon and two-phonon types. Particularly interesting is the decomposition of the $4^+_{2\text{-}ph}$ state which reveals a prominently large 4^+_1 component. From Fig. 7 it can be seen that the two one-phonon-like states, 2^+_1 and 4^+_2, have as the major component the corresponding QRPA phonon. Anharmonicities show up as mixing of two-QRPA-phonon components into these states, the components $(2^+_1 2^+_1)_J$ and $(2^+_1 4^+_1)_J$ being the largest ones of these anharmonicities.

In Fig. 8 we show the relation between the QRPA and MAVA energies. As one can see, the MAVA energies follow quite smoothly the corresponding QRPA energies. However, the MAVA energies are lowered by few hundred keV compared to the QRPA energies. Notable exception is the 4^+_2 state: for $A=98$ the MAVA energy is almost the same as the corresponding QRPA energy. For $A=100$ energies are separated by about 200 keV and for $A>100$ the separation be-

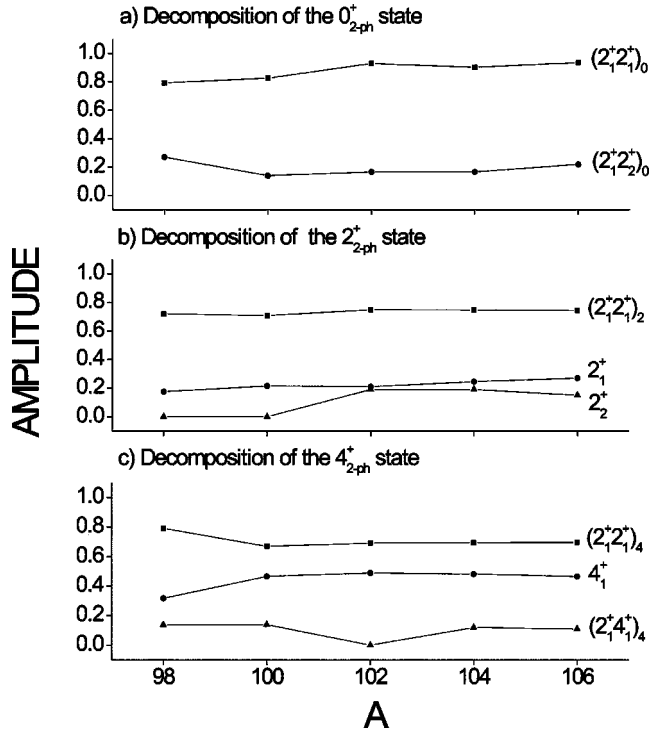

FIG. 6. Decomposition of the calculated wave function into one- and two-QRPA-phonon amplitudes for the $0^+_{2\text{-}ph}$ state (panel a), $2^+_{2\text{-}ph}$ state (panel b), and $4^+_{2\text{-}ph}$ state (panel c) for the discussed $^{98-106}$Ru nuclei.

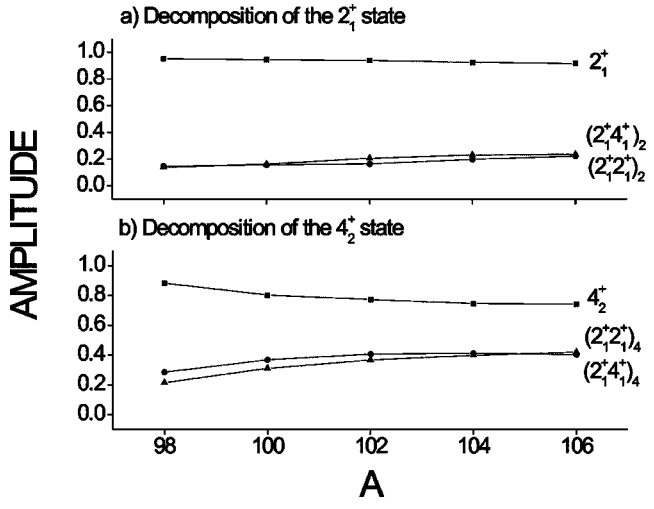

FIG. 7. Decomposition of the calculated wave function into one- and two-QRPA-phonon amplitudes for the 2^+_1 state (panel a) and 4^+_2 state (panel b) for the discussed $^{98-106}$Ru nuclei.

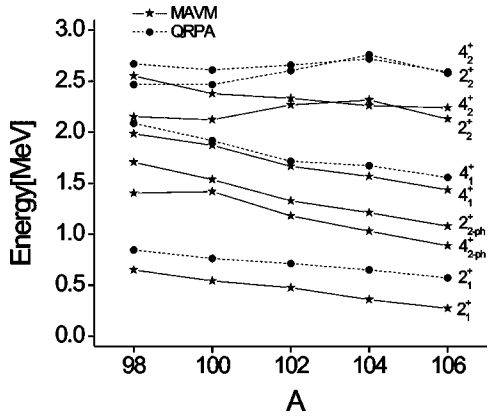

FIG. 8. Evolution of the energies for the QRPA (dots) 2_1^+, 4_1^+, 2_2^+, 4_2^+ phonons, for the corresponding MAVA states (stars) containing the mentioned QRPA phonons as main component, and for the two-phonon states of the MAVA for the discussed $^{98-106}$Ru nuclei.

comes larger, being about 300 keV. The MAVA 2^+ and 4^+ two-phonon states seem to follow the trend of the QRPA 2_1^+ state as one would expect.

In Tables II and III we summarize the experimental information about the values of the ratio

$$R_{if}(E2) = \frac{B(E2; J_i^+ \to J_f^+)}{B(E2; 2_1^+ \to 0_1^+)} \tag{3.1}$$

for the ruthenium isotopes under discussion. The relevant theoretical results concerning the five lowest calculated states have also been given. Choosing the experimental 0_2^+, 2_2^+, and 4_1^+ states to correspond to our calculated triplet of anharmonic two-phonon-like states leads to the numbers of Tables II and III. For the ruthenium isotope $A=106$ no experimental data are available and no conclusions about the correspondence can be drawn.

Let us look closer at the correspondence of the calculated and experimental $B(E2)$ values of Tables II and III. From Table II one can see that for the isotope $A=98$ all the calculated $B(E2)$ values correspond extremely well to the experimental data. Even the very weak transition $2_{2\text{-}ph}^+ \to 0_1^+$ is very well reproduced. This means that ^{98}Ru can be considered to be a good anharmonic vibrator of (nearly) spherical shape. For the other rutheniums the situation is worse. From Tables II and III one can see that judging by the transitions from the two-phonon-type states to the 2_1^+ state one can say that $^{100-106}$Ru seem to be less pure vibrators than the theory predicts. First we note that for the transitions $0_{2\text{-}ph}^+ \to 2_1^+$ and $2_{2\text{-}ph}^+ \to 2_1^+$ in these nuclei the theoretical value is always much larger than the experimental one. For the transition $4_{2\text{-}ph}^+ \to 2_1^+$ the theoretical value is slightly too large in the case of ^{100,102}Ru, whereas in the case of ^{104}Ru it is slightly too small. For the very weak $2_{2\text{-}ph}^+ \to 0_1^+$ transition the theoretical $B(E2)$ values are somewhat too large but still quite acceptable. From the theoretical point of view this transition can proceed mainly through the mixing of the lowest 2^+ phonon of the QRPA into the $2_{2\text{-}ph}^+$ state of the MAVA. The square of this mixing amplitude determines the theoretical $B(E2)$ value for this transition.

It is instructive to look at the evolution of the vibrational excitations to rotational ones within the Sheline-Sakai scheme [44]. In this scheme the two-phonon 0^+, 2^+, and 4^+ states of the (an)harmonic spherical (or nearly spherical) vibrator evolve to the corresponding rotational states of a well-deformed rotator nucleus. These states are the 0^+ β-band head, 2^+ γ-band head, and the 4^+ member of the ground-state rotational band. On the rotational regime the 2^+ member of the ground-state band would correspond to the first 2^+ vibrational state of the (an)harmonic vibrator, and the γ-decay feeding of this state (called 2_1^+ state below) from the above mentioned 0^+, 2^+, and 4^+ states can be classified into interband and intraband transitions. The intraband transition from the 4^+ to the 2_1^+ state is typically strong, the corresponding $B(E2)$ being 1.43 times the $B(E2)$ of the 2_1^+ to ground state transition in the limit of very large deformations, reproducing the Alaga rule [45]:

$$\frac{B(E2; 4_g^+ \to 2_g^+)}{B(E2; 2_g^+ \to 0_g^+)} = 25 \begin{pmatrix} 4 & 2 & 2 \\ 0 & 0 & 0 \end{pmatrix}^2 = 1.43. \tag{3.2}$$

On the other hand, the interband $2^+ \to 2_1^+$ and $0^+ \to 2_1^+$ transitions are very weak, even vanishing at the limit of large deformations.

In the IBA-1 model the above described transition from the harmonic vibrator to the deformed rotor through anharmonic vibrator regime corresponds to transition from the U(5) symmetry to the SU(3) symmetry along the base of the Casten triangle. The anharmonicities of the MAVA can also be viewed as deviations from the base of the triangle towards the γ-unstable O(6) top of the triangle. In any case, the anharmonicities contained in the MAVA are able to cover a considerable part of the Casten triangle, missing only the deformed regions towards the SU(3) corner of the triangle.

Considering the γ decays of the two-phonon-like states in the $^{100-106}$Ru nuclei from the point of view of the interband and intraband transitions, one can say that the experimental data would point to increasing rotational character of these nuclei as function of the mass number. This observation is based on the weakening of the interband type of transitions and the persistence of the strong intraband type of transitions along the isotopic chain. This behavior cannot be reproduced by the MAVA for the $^{102-106}$Ru nuclei, since MAVA tends to produce rather strong interband type of transitions. It seems, however, that the nucleus ^{100}Ru is described moderately well by the MAVA, and thus ^{100}Ru would be at a "phase-transition point" between the anharmonic vibrator region and the deformed rotor region. Thus, according to our calculations, ^{98}Ru seems to be an anharmonic vibrator and $^{102-106}$Ru (quasi)rotors, ^{100}Ru being a "transitional" nucleus between these two regimes. Related to this, an interesting discussion about the possible phase-transition point in the $^{98-110}$Ru chain has been carried out in Ref. [20], based on the work of Iachello in Ref. [21]. In Ref. [20] the critical point symmetry $E(5)$, supposed to lie midway between the spherical vibrator limit U(5) and the γ-unstable limit O(6), was sought for. The

^{104}Ru nucleus was proposed to lie at this phase-transition point. Similarly, the nucleus ^{102}Pd was proposed to be an $E(5)$ nucleus in Ref. [46].

All these observations are interesting from the point of view of the β-decay and double-β-decay feeding of the ^{100}Ru nucleus, since in Refs. [47–49] it was verified that it is impossible to describe the β and double-β feeding of ^{100}Ru within a simple spherical QRPA approach using simple harmonic wave functions for the two-phonons-like states. These matters will be discussed within the MAVA in future publications.

IV. CONCLUSIONS

We have presented results of calculations of the properties of the even-even $^{98–106}$Ru isotopes, in particular the feasibility of certain states to be interpreted as two-phonon states of vibrational origin, and found in many cases good agreement between our calculations and experiment. The simple microscopic formalism, which we have applied, is based on a large single-particle valence space and a realistic nuclear Hamiltonian using phenomenologically renormalized two-body interaction based on the Bonn one-boson-exchange G matrix. The used theoretical formalism naturally embraces vibrational degrees of freedom starting from the QRPA collective phonons. The above mentioned nuclear Hamiltonian is used to introduce anharmonicities into the description of the low-lying excited states leading to dynamical splitting of the energies of the two-phonon vibrational states. At the same time the Hamiltonian is also allowed to mix the one-phonon and two-phonon collective degrees of freedom.

There were mainly two reasons for studying the Ru isotopes: First there are several papers available about ruthenium isotopes, both theoretical and experimental, and second within the isotopic chain of rutheniums there are experimental indications of shape transitions. According to our calculations ^{98}Ru seems to be an anharmonic vibrator and $^{98–106}$Ru more or less well defined quasirotors, ^{100}Ru being a transitional nucleus between these two regimes. This view was supported by the comparison of the calculated $B(E2)$ values with the experimental data. One can say that the MAVA technique is able to bring a new viewpoint to the study of this mass region and could further be used for studying the properties of other isotopic mass chains in this or other mass regions.

ACKNOWLEDGMENT

This work was supported by the Academy of Finland under the Finnish Center of Excellence Program 2000-2005 (Project No. 44875, Nuclear and Condensed Matter Program at JYFL).

[1] R. F. Casten and N. V. Zamfir, Phys. Rep. **264**, 81 (1996).
[2] M. Baranger, Phys. Rev. **120**, 957 (1960).
[3] D. J. Rowe, *Nuclear Collective Motion* (Methuen, London, 1970).
[4] P. Ring and P. Schuck, *The Nuclear Many-Body Problem* (Springer-Verlag, Berlin, 1980).
[5] A. Insolia, N. Sandulescu, J. Blomqvist, and R. J. Liotta, Nucl. Phys. **A550**, 34 (1992).
[6] N. Sandulescu, A. Insolia, B. Fant, J. Blomqvist, and R. J. Liotta, Phys. Lett. B **288**, 554 (1992).
[7] V. G. Soloviev, *Theory of Atomic Nuclei: Quasiparticles and Phonons* (IOP, Bristol, 1992).
[8] S. Drozdz, S. Nishizaki, J. Speth, and J. Wambach, Phys. Rep. **197**, 1 (1990).
[9] D. S. Delion and J. Suhonen, Phys. Rev. C **67**, 034301 (2003).
[10] F. Iachello and A. Arima, *The Interacting Boson Model* (Cambridge University Press, Cambridge, 1987).
[11] J. H. Hirata, S. Salém-Vasconcelos, M. J. Bechara, L. C. Gomes, and O. Dietzsch, Phys. Rev. C **57**, 76 (1998).
[12] R. F. Casten, W. Frank, and P. Von Brentano, Nucl. Phys. **A444**, 133 (1985).
[13] A. K. Vlasnikov and V. M. Mikhailov, Izv. Akad. Nauk SSR Ser. Fiz. Mat. Nauk **53**, 58 (1989).
[14] P. Van Isacker and G. Puddu, Nucl. Phys. **A348**, 115 (1980).
[15] A. Giannatiempo, A. Nannini, P. Sona, and D. Cutoiu, Phys. Rev. C **52**, 2969 (1995).
[16] D. D. Warner and R. F. Casten, Phys. Rev. C **28**, 1798 (1983).
[17] D. Bucurescu, G. Cata, D. Cutoiu, G. Constantinescu, M. Ivascu, and N. V. Zamfir, Z. Phys. A **324**, 387 (1986).
[18] J. Stachel, P. Van Isacker, and K. Heyde, Phys. Rev. C **25**, 650 (1982).
[19] R. F. Casten and D. D. Warner, Rev. Mod. Phys. **60**, 389 (1988).
[20] A. Frank, C. E. Alonso, and J. M. Arias, Phys. Rev. C **65**, 014301 (2001).
[21] F. Iachello, Phys. Rev. Lett. **85**, 3580 (2000).
[22] F. Iachello, Phys. Rev. Lett. **87**, 052502 (2001).
[23] J. Kern, P. E. Garrett, J. Jolie, and H. Lehmann, Nucl. Phys. **A593**, 21 (1995).
[24] A. Bohr and B. R. Mottelson, *Nuclear Structure* (Benjamin, New York, 1969), Vol. I.
[25] K. Holinde, Phys. Rep. **68**, 121 (1981).
[26] J. Suhonen, T. Taigel, and A. Faessler, Nucl. Phys. **A486**, 91 (1988).
[27] J. Suhonen, Nucl. Phys. **A563**, 205 (1993).
[28] G. Audi and A. H. Wapstra, Nucl. Phys. **A565**, 1 (1993).
[29] K. Zajaç, L. Próchniak, K. Pomorski, S. G. Rohoziński, and J. Srebrny, Nucl. Phys. **A653**, 71 (1999).
[30] A. J. Singh and P. K. Raina, Phys. Rev. C **53**, 1258 (1996).
[31] A. Bharti, R. Devi, and S. K. Khosa, J. Phys. G **20**, 1231 (1994).
[32] D. Troltenier, J. A. Maruhn, W. Greiner, V. Velazquez Aguilar, P. O. Hess, and J. H. Hamilton, Z. Phys. A **338**, 26 (1991).
[33] H. Aiba, Prog. Theor. Phys. **84**, 908 (1990).
[34] A. Frank, Phys. Rev. C **39**, 652 (1989).
[35] V. K. Datta, V. P. Varshney, K. K. Gupta, and S. P. Sud, J.

Phys. Soc. Jpn. **54**, 901 (1985).
[36] K. Heyde, P. Van Isacker, M. Waroquier, and J. Moreau, Phys. Rev. C **29**, 1420 (1984).
[37] K. Weeks and T. Tamura, Phys. Rev. C **22**, 888 (1980).
[38] B. Singh, Nucl. Data Sheets **84**, 565 (1998).
[39] B. Singh, Nucl. Data Sheets **81**, 1 (1997).
[40] J. Blachot, Nucl. Data Sheets **64**, 1 (1991).
[41] D. De Frenne and E. Jacobs, Nucl. Data Sheets **72**, 1 (1994).
[42] D. De Frenne and E. Jacobs, Nucl. Data Sheets **83**, 535 (1998).
[43] J. Kotila, J. Suhonen, and D. S. Delion, Phys. Rev. C **68**, 014307 (2003).
[44] R. K. Sheline, Rev. Mod. Phys. **32**, 1 (1960); M. Sakai, Nucl. Phys. **A104**, 301 (1967).
[45] G. Alaga, K. Alder, A. Bohr, and B. R. Mottelson, Mat. Fys. Medd. K. Dan. Vidensk. Selsk. **29**, 9 (1955).
[46] N. V. Zamfir *et al.*, Phys. Rev. C **65**, 044325 (2002).
[47] A. Griffiths and P. Vogel, Phys. Rev. C **46**, 181 (1992).
[48] O. Civitarese and J. Suhonen, Phys. Rev. C **47**, 2410 (1993).
[49] J. Suhonen, Nucl. Phys. **A700**, 649 (2002).